J. Chem. Sci. (2024) 136:44
https://doi.org/10.1007/s12039-024-02279-1

REGULAR ARTICLE

Switching the regio-, stereo- and enantioselectivity in L-proline catalyzed asymmetric Mannich reaction: A case study of H-acceptor and H-donor solvents

PARIMAL J MALIEKAL[a], ARATI S GAVALI[a], PRIYANKA PATEL[b] and PURAV M. BADANI[a,*]

[a]Department of Chemistry, University of Mumbai, Vidyanagari Santacruz, Mumbai 400098, India
[b]Atharva College of Engineering, Malad West, Mumbai 400095, India
*Corresponding Author. E-mail: pmbadani@chem.mu.ac.in

MS received 10 January 2024; accepted 17 March 2024

Abstract. We report the detailed mechanistic insights of L-proline catalyzed, solvent-controlled, regioselective Mannich reaction. Different solvation models were employed to understand the formation of critical intermediates. The seminal difference in the nature of H-acceptor solvents and H-donor solvents leads to variation in the attachment site on the reactant molecule. Our calculations suggest that the H-acceptor solvent exhibits selective non-covalent interaction with α-hydrogen atoms of the iminium group, facilitating the reactivity at the more hindered site, which results in the formation of a branched isomer. On the other hand, the H-donor solvent preferentially binds to the carboxylate group, thus enabling the reactivity to proceed from the less hindered carbon chain, leading to a linear isomer. The above distinct interactions force a regioselective generation of enamines. Thus, the iminium ion's site-specific solvent interaction has been observed to cause a switch in the regioselectivity. These enamines subsequently react with cyclic ketone to produce Mannich base with excellent enantioselectivity (>99%ee).

Keywords. Mannich base; enantioselectivity; H-acceptor; H-donor; regioselectivity; L-proline.

1. Introduction

The foray of L-proline as an alternative strategy to the domain of metal-catalyzed chiral reactions gathered rapid recognition of its natural availability, eco-friendly, and cost-effective attributes.[1] The burgeoning applications of L-proline conspicuously prove the efficacy of this organocatalyst in the flourishing field of asymmetric organocatalysis.[2] The versatility offered by L-proline in the realm of organic chemistry has triggered much attention among chemists.[3] Extensive literature is available regarding the L-proline catalyzed enamine formation.[4–7] The formation of enamine constitutes the preliminary step of prominent organic reactions, such as aldol reaction, mannich reaction, etc.[8,9] The enamine catalysis is considered to be among the main activation mechanisms in organocatalysis and has emerged as a particularly potent technique for the enantioselective α-functionalization of carbonyl compounds.[9,10]

The earliest instances of enamine formation were found in the experimental work of Hajos *et al.* and List *et al.* which was subsequently followed by the theoretical work of Houk and co-workers.[11–14] Following are the pathways suggested for the formation of enamine. According to the mechanism proposed by List, the reaction commences with the forming of a carbinolamine intermediate, followed by the loss of a water molecule to produce a zwitterionic intermediate, which proceeds through an intramolecular proton transfer to produce enamine.[12,13] In the second pathway, the carboxylic acid group of L-proline stabilizes the formal charges in the transition state and increases the interaction between the reacting partners through hydrogen bonding.[14–16] This particular mechanism is energetically feasible relative to the formation of the carbinolamine intermediate. Houk and co-workers

Supplementary Information: The online version contains supplementary material available at https://doi.org/10.1007/s12039-024-02279-1 and https://www.ias.ac.in/chemsci.

Published online: 06 June 2024

have computationally rationalized that the enamine process catalyzed by carboxylic acid is preferred by around 30 kcal mol^{-1} over the mechanism involving the zwitterionic form of the enamine. Consequently, this energetically viable approach is referred to as the Houk–List pathway. Seebach *et al.* proposed an alternate oxazolidinone pathway, which quickly became prominent as oxazolidinones could be detected experimentally in various circumstances.[17] Later, Sunoj and co-workers probed the factors affecting the stereoselectivity caused by the enamines and oxazolidinones. They observed that the stereoselectivities are linked to the electrophile's preferred approach during the subsequent formation of the C–C bond between the enamine and the imine, leading toward the Mannich base formation.[18] The computationally derived results of the oxazolidinone-led mechanism resulted in different diastereomers compared to the experimentally observed products, while the enamine-led mechanism produced the diastereomers as obtained experimentally.[19] Similarly, Gschwind and co-workers investigated the subtleties of enamine production.[20] They investigated the rate of enamine production in basic additives, and the results were supported by theoretical analysis. According to their findings, the Houk-List pathway is preferable to Seebach's hypothesized oxazolidinone pathway. Based on energetics and experimental observations, there is a general consensus that the mechanism proposed by Houk and List operates for the enamine formation, and the Seebach mechanism for enamine formation can be ruled out.[18–20]

Experimental parameters alter the effectiveness of organocatalytic reactions. For instance, the choice of appropriate solvent causes a variation in the reaction rate, enantioselectivity, regioselectivity, etc.[5] The effect of acids and hydrogen bond acceptors on the reaction rates and equilibria of enamine production have been well investigated.[5] Acids can speed up the process, but they do not alter the equilibrium of the reaction. For instance, when p-toluene sulfonic acid was added to $CDCl_3$, the enamine formation using pyrrolidine and cyclohexanone was enhanced. The hydrogen bond acceptors, for example, dimethyl sulfoxide (DMSO), support the production of enamine through their potent hydrogen bonding interaction with the water produced during the process, unlike solvents such as benzene.[5] High enantioselectivity is observed in polar aprotic organic solvents like DMSO and dimethylformamide (DMF) in the case of proline-catalyzed Mannich reactions.[19–21] Additionally, the pioneering contribution from Barbas has revealed that amine-derived chiral catalysts induce excellent enantiocontrol in the presence of excess water in an aldol reaction, and there is no requirement for acid additives; this is because the reactants are more miscible in water.[22]

The formation of regioisomers based on the use of solvent in the case of enamines proves to be effective. The regio-enantioselectivity of the Mannich base holds significant potential in the formulation of precursors used in the pharmaceutical industries. Therefore, multiple research groups exploit the factors that fetch the best output from Mannich-type reactions. Unsurprisingly, researchers have been concentrating their efforts in recent years on synthesizing cyclic imines and improving the efficiency of the Mannich process.[23] The formation of branched product in DMSO and linear product in $CHCl_3$ in a reaction between benzoxazinone and 2-hexanone using L-proline is shown in Scheme 1.[24] The role of solvent in such reactions is unclear and not well explored, which thereby caused curiosity within us to conduct a comprehensive mechanistic analysis to link the experimental study and interpret the experimental data.[25–27] This paper should be useful in exploring the role of solvent in controlling the regio-, stereo-, and enantioselective organic synthesis and, hence, in the pragmatic design and development of new organic synthesis.

2. Methodology

The Gaussian 09 quantum chemistry software was used to perform the geometry optimization of all reactants, intermediates, transition states, and products in this study.[28] The ωB97X-D functional in conjugation with the 6-311G(d,p) basis set predicts energy estimates that are in close agreement with the existing experimental data for numerous reactions.[29–31] As a result, all of the computations in this paper were done at the same theoretical level. The effect of solvent on the reaction mechanism was evaluated by performing the calculations using the above-mentioned theory and an implicit CPCM model at the same level of theory.[32] The explicit solvation model was employed in the critical transition state (TS) to study the interaction of solvents and their effect on the reaction process. A single imaginary frequency was observed in all of the transition structures generated, and this was confirmed using an intrinsic reaction coordinate (IRC) scan to ensure that the TS interlinks the reactant and intermediate/product. The supporting information (SI) includes cartesian coordinates for the optimized structures of the reactants, transition structures, and

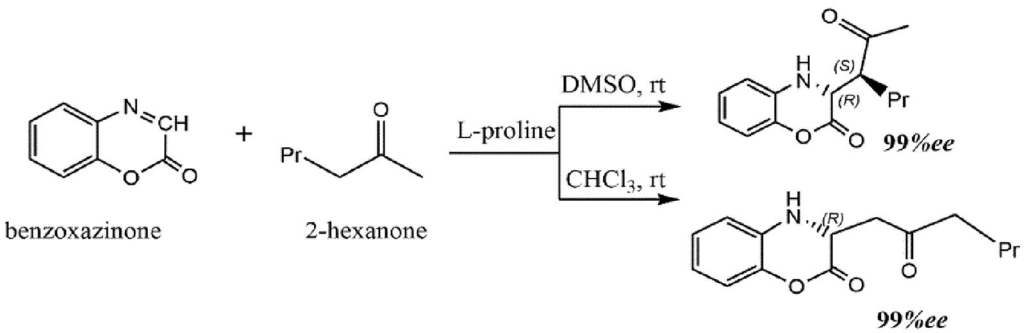

Scheme 1. Branched and linear Mannich bases formed via the regioselective organocatalyzed Mannich reaction between benzoxazinone and 2-hexanone in the presence of DMSO and $CHCl_3$.

intermediates (Figures S1–S40 of SI). Multiwfn was used to produce the NCI plot, enabling us to study the interaction between the solute and the solvent,[33] and VMD was used to improve the visualization of structures exhibiting non-covalent interactions.[34]

3. Results and discussion

Based on the suggested mechanism by multiple research groups, as discussed in Section 1, the energetics of the enamine formation involved in the present reaction system are discussed herein.[12,18–20,35–37] The Houk-List pathway involves the nucleophilic attack of L-proline onto the carbonyl of the ketone (requires 10.35 kcal mol^{-1}), leading to proton abstraction from the carboxylic acid group.[38] A concerted mechanism was observed for the above nucleophilic attack, and proton abstraction occurs via TS **(1-2)**$^{‡'}$ to form **2′**. The carboxylic anion in **2′** abstracts the proton from the ammonium cation, forming **2**, and the reaction proceeds with the loss of a water molecule, as shown in Scheme 2.[20,39] In the List mechanism, the reaction involves the concerted nucleophilic attack of L-proline onto the carbonyl carbon of the ketone followed by abstraction of proton attached to nitrogen of L-proline by the carboxylate ion, requiring 39.61 kcal mol^{-1} via TS **(1-2)**‡ to form **2**.[12]

This is followed by the loss of a water molecule to yield a zwitterionic intermediate with subsequent intramolecular proton transfer, resulting in the formation of enamine **4/4′**. The formation of a zwitterionic intermediate is confirmed through charge analysis employing the Charges from Electrostatic Potentials using a Grid-based method (ChelpG) and natural bond orbital (NBO) analysis (see Table S1 of SI).[40–42] The formation of enamine isomers was crucially considered as it paves the way for the regioselective generation of the final products. The energetics indicate that the Houk-List pathway is feasible. This observation is

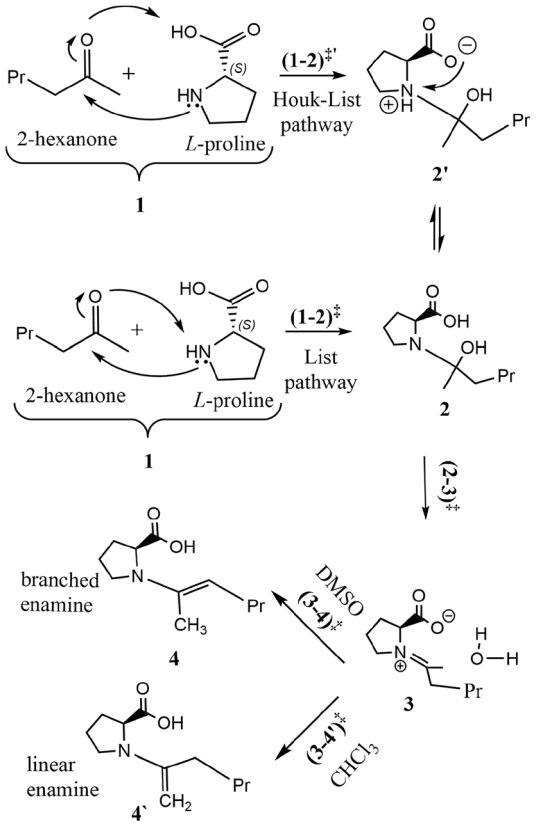

Scheme 2. Formation of enamine using DMSO and $CHCl_3$ resulting in branched and linear isomer.

in line with the observations of other research groups.[18,20]

3.1 *Mechanistic insights of the formation of linear and branched enamines*

3.1.1 *Energetics of enamine formation in the gas phase*: The stereochemistry of the final product is largely influenced by the isomerization of enamine. In reaction Scheme 2, intermediate **3** can undergo rearrangement to form branched (**4**) or linear isomers

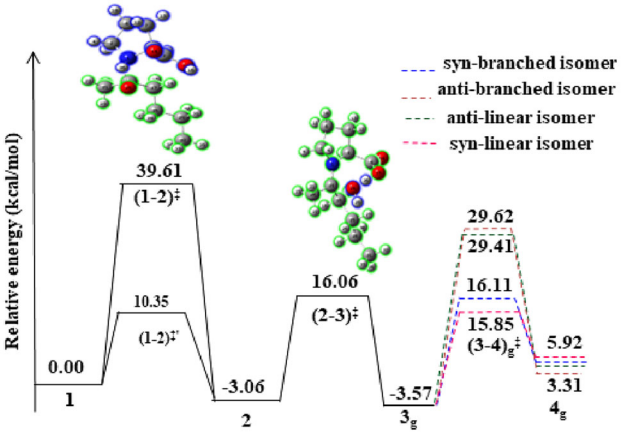

Figure 1. A potential energy surface for the formation of enamine using electronic energies performed at 6-311G(d,p) level of theory using ωB97X-D functional in the gas phase. The blue dotted line represents the formation of a syn-branched isomer; the brown dotted line represents the formation of an anti-branched isomer; the green dotted line represents the formation of an anti-linear isomer, and the pink dotted line represents the formation of a syn-linear isomer, respectively.

(**4′**). The generation of branched and linear isomers of enamine **4/4′** from the iminium ion via α-proton transfer was examined in the gas phase. It becomes pivotal to compute the energy barrier of all possible isomers to identify the most feasible reaction pathway leading to the generation of the product. The energy barrier for the formation of syn/anti-linear and syn/anti-branched isomers and the relative stability of each isomer have been listed in Table S2. Figure 1 depicts a potential energy surface of reaction Scheme 2. It can be seen that the anti-branched enamine is thermodynamically stable but requires the highest activation energy. Thus, the kinetically favored syn-linear enamine is formed, which subsequently undergoes conversion via a low energy-assisted rotational transition across the C–N bond to generate the anti-linear enamine. This suggests that the anti-linear enamine is the favored product, which is in line with the experimentally obtained product in $CHCl_3$. However, in DMSO, the product obtained is anti-branched, which could not be rationalized through gas phase calculations. Hence, to investigate the role of solvent, we have subsequently performed the calculations using an implicit solvation model.

3.1.2 *Energetics of enamine formation using implicit solvation model*: To evaluate the energetics for the effect of solvent on enamine formation, we employed a CPCM model at ωB97X-D with 6-311G(d,p) level of theory.[29–32,43] The energies were computed in two different solvent environments, i.e., DMSO and $CHCl_3$ (see Table S3). Figures S41 and S42 represent the potential energy surface in the presence of DMSO and $CHCl_3$, respectively. It is evident that the anti-branched product is thermodynamically stable in both DMSO and $CHCl_3$. However, the energy barrier required for the formation of an anti-branched product is large in DMSO (35.21 kcal mol^{-1}) and $CHCl_3$ (33.64 kcal mol^{-1}). Hence, the formation of the branched product is highly unfavorable in both solvents. As per kinetic consideration, a syn-linear and syn-branched product is expected to be formed. This is in sharp contrast to experimental findings wherein the anti-branched and anti-linear product is formed in the presence of DMSO and $CHCl_3$, respectively.[24] This strongly suggests there is solvent-specific interaction behind the regioselectivity, which needs to be investigated. Therefore, we continued to study the role of solvent using an explicit solvation model.

3.1.3 *Energetics of enamine formation using explicit solvation model*: We probed the mechanism of enamine production using an explicit solvation model to check for any difference in enamine formation preference between DMSO and $CHCl_3$. The electronic energies used to account for the formation of these enamine isomers are depicted in Table 1. In the presence of DMSO, the syn-branched enamine has the lowest energy barrier for formation, and thus, the branched isomer gets formed in preference to the linear enamine. Likewise, in the presence of $CHCl_3$, the syn-linear enamine has a minimum energy barrier of formation, so the linear isomer is formed over the branched enamine.

From Table 1, we can interpret that in the DMSO environment, the lowest energy barrier was observed for the formation of branched-syn enamine, but the anti-branched enamine is more thermodynamically stable than the syn-branched enamine. Therefore, the syn-branched enamine formed as the kinetic product later rotates to form the thermodynamically stable anti-branched enamine, requiring 7.43 kcal mol^{-1}. This step has a substantially lower energy requirement as compared to the reaction barrier involving direct anti-branched enamine formation (17.61 kcal mol^{-1}).[44] Hence, the former pathway is the feasible approach towards forming anti-branched enamine in DMSO. Figure 2(a) illustrates the energies required to form all possible enamine isomers. Figure 2(b) depicts the relaxed rotation potential between syn- and anti-enamine using DMSO as an explicit

Table 1. Theoretically, estimated energies for the formation of enamine using explicit solvation model in the presence of DMSO and $CHCl_3$ at ωB97X-D/6-311G(d,p) level of theory.

	DMSO				$CHCl_3$			
	Linear		Branched		Linear		Branched	
	syn	anti	syn	anti	syn	anti	syn	anti
Energy barrier (kcal mol^{-1})	4.91	32.69	3.36	17.61	18.91	33.17	19.76	31.44
Enamine (kcal mol^{-1})	−10.06	−3.99	−15.91	−16.62	−2.83	−4.65	0.28	0.17

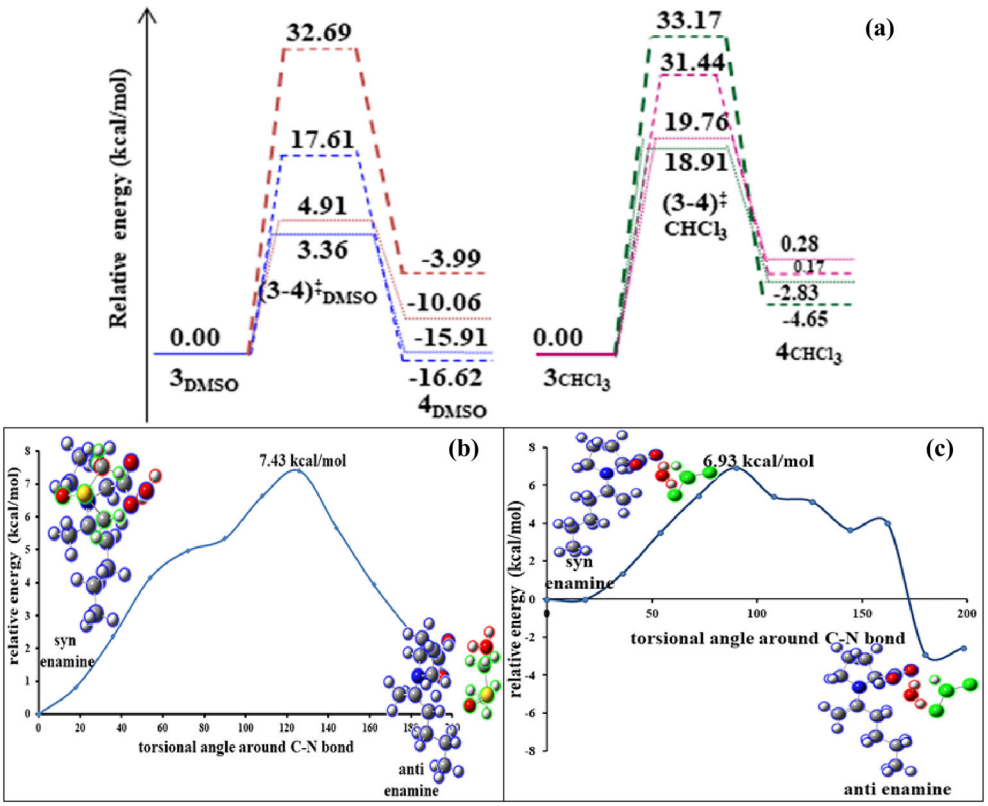

Figure 2. (a) A potential energy surface for the formation of enamine using electronic energies obtained at ωB97X-D/6-311G(d,p) level of theory. The brown dash line represents the formation of an anti-linear isomer in DMSO, the brown dotted line represents the formation of a syn-linear isomer in DMSO, the blue dash line represents the formation of anti-branched isomer in DMSO, the blue dotted line represents the formation of syn-branched isomer in DMSO, the green dash line represents the formation of anti-linear isomer in $CHCl_3$, the green dotted line represents the formation of syn-linear isomer in $CHCl_3$, the pink dash line represents the formation of anti-branched isomer in $CHCl_3$ and the pink dotted line represents the formation of syn-branched isomer in $CHCl_3$, respectively, using ωB97X-D/6-311G(d,p) level of theory (explicit solvation); (b) The C–N bond rotation potential energy performed using ωB97X-D/6-311G(d,p) for branched syn-enamine to anti-enamine in presence of DMSO; and (c) The C–N bond rotation of linear syn-enamine to anti-enamine in presence of $CHCl_3$.

solvent. Similarly, in the presence of $CHCl_3$, as shown in Figure 2(c), the lowest energy barrier for forming linear-syn enamine was observed at 18.91 kcal mol^{-1}. Nonetheless, the anti-linear enamine is thermodynamically more stable than the syn-linear enamine. As a result, the kinetic product is syn-linear enamine, which then rotates to form the thermodynamically stable anti-linear enamine with a rotation barrier of 6.93 kcal mol^{-1}. This barrier is significantly lower than the reaction barrier for anti-enamine production (31.44 kcal mol^{-1}).[45] We can confirm this as the preferred pathway for forming anti-linear enamine in $CHCl_3$.

Our calculations suggest that a more substituted enamine isomer forms preferentially in DMSO (i.e.,

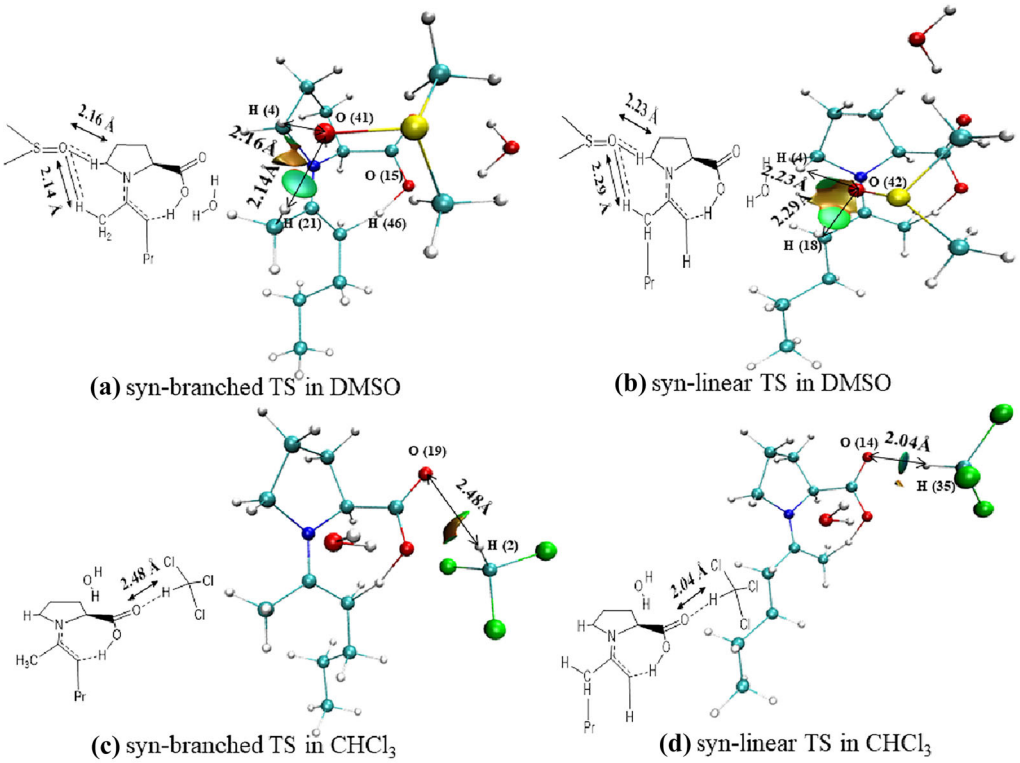

Figure 3. NCI plot showing the interaction of solute in the presence of DMSO and $CHCl_3$ in TS $(3\text{-}4)^{‡}$ and $(3\text{-}4')^{‡}$, respectively.

H-acceptor solvent), while a less substituted enamine isomer forms preferentially in $CHCl_3$ (i.e., H-donor solvent). Based on our calculations, we could envisage that the formation of enamine isomers differs depending on the solvent environment, and so, to validate this, we performed the analysis using two H-donor and two H-acceptor solvents to gain a deeper understanding and to validate this factor as a cause for the induced regioselectivity. We employed tetrahydrofuran (THF) and DMF as H-acceptor solvents and dichloromethane (CH_2Cl_2) and chloromethane (CH_3Cl) as H-donor solvents. In the case of H-acceptor solvents like THF and DMF, the syn-branched enamine formation is favored over syn-linear enamine. The energy barrier for syn-branched enamine was lower by 1.41 and 1.99 kcal mol^{-1} in the presence of THF and DMF, respectively. On the other hand, the formation of syn-linear enamine was favored in the presence of H-donor solvents. Solvents such as CH_2Cl_2 and CH_3Cl favored the syn-linear TS over the branched TS by 1.77 and 0.07 kcal mol^{-1}, respectively. In general, the above calculations suggest that the H-acceptor solvent forms a branched isomer, and the H-donor solvent leads to the formation of a linear isomer, thereby confirming that the regioselectivity is induced due to the solvent. The interaction of solvents has been critically explored in the next part to gain better insights into the role of solvents in stabilization.[46] Such stabilizing interactions would have gone undiscovered if our study had not utilized an explicit solvation model.[47]

3.1.4 *Non-covalent interactions between solvent and enamine*: As discussed in the earlier section, the role of solvent during the current reaction stage is extremely vital in forming the regioselective enamines. DMSO and $CHCl_3$ are the two solvents employed in this study, so we delved into the interactions caused by these solvents over the solute. DMSO acts as an H-acceptor due to the presence of lone pairs on its two oxygen atoms.[48] On the other hand, the three chlorine atoms in $CHCl_3$ exert a -I effect, which generates a large fractional positive charge (0.216) on the H atom.[49] Hence, $CHCl_3$ behaves as an H-donor (see Figure S43)—the solvent-dependent stabilization results in the generation of regioselective isomers. The interaction of the solvent with solute in the TS $\mathbf{(3\text{-}4)}^{‡}$ and $\mathbf{(3\text{-}4')}^{‡}$ are presented in Figure 3.

DMSO can approach the iminium ion by maintaining a distance from the carboxylate ion to minimize repulsive forces. Further, there are two probable modes of interaction of DMSO with iminium ion, which can generate either branched or linear enamine.

To form branched enamine, DMSO needs to orient itself away from the larger C chain and exhibit stronger C–H···O interaction of 2.16 Å between O(41) and H(4) and 2.14 Å between O(41) and H(21) (Figures 3a, S22 and S23). Because of the involvement of H(4) and H(21) in H-bonding, their chemical reactivity is hindered. This forces the carboxylate oxygen, i.e., O(15), to abstract 46(H), forming branched enamine. To form linear enamine, DMSO needs to orient itself towards the larger C chain, leading to C–H···O interaction with 2.23 Å between O(42) and H(4) and 2.29 Å between O(42) and H(18) (Figure 3b). These non-covalent interactions are weaker than the former due to steric reasons. Overall, this results in the generation of relatively stable TS for forming branched enamine over linear enamine when DMSO is used as a solvent.

Likewise, as discussed in Section 3.3.3, the H-acceptor solvents like DMF and THF are likely to produce the branched enamine in preference to the linear enamine. The mode of interaction between iminium ion and respective solvent molecules (DMF, THF) is identical to DMSO. That is, (DMF/THF) approaches iminium ions by maintaining maximum distance from carboxylate ions to minimize the repulsive electrostatic interactions. As discussed earlier, the carboxylate ion arm abstracts a proton that is not involved in non-covalent interactions, resulting in the preferential generation of branched enamine (see Figures S44 and S45).

In sharp contrast to H-acceptor solvents, the H-donor solvents, like $CHCl_3$, approach the iminium ion such that it is in close proximity to the carboxylate ion, as it offers attractive dispersive interactions between the H atom of $CHCl_3$ and the carboxylate ion. As seen in the case of H-acceptor solvents, the H-donor solvents also show two modes of interaction with iminium ions, forming either branched or linear isomers. The branched isomer shows a hydrogen bond (HB) length of 2.48 Å (Figure 3c), whereas the linear isomer (Figure 3d) exhibits a stronger (HB) of 2.04 Å when $CHCl_3$ was used as solvent. The stabilization in linear isomer is due to the lower steric crowding as HB is far from the larger C chain. The branched isomer has a relatively larger steric crowding, where the HB is close to the larger C chain. This stabilization of HB in H-donor solvent leads to the preferential formation of linear isomer over branched isomer. The weak HB in branched isomer results from the repulsive forces caused by the comparatively larger C chain over the hydrogen of $CHCl_3$. The syn-linear TS in $CHCl_3$ exhibits stronger HB as there are no repulsive forces since the HB is far from the larger C chain. Likewise, in the case of CH_2Cl_2, the branched isomer exhibits HB of 2.29 Å, and the linear isomer (Figure S46a) shows hydrogen bonding (HB) of 2.21 Å, thereby providing stabilization compared to the branched isomer. The weak HB in branched isomer results from the repulsive forces caused by the comparatively larger C chain over the hydrogen of CH_2Cl_2. The syn-linear TS in CH_2Cl_2 (Figure S46b) exhibits stronger HB as there are no repulsive forces since the HB is far from the larger C chain. Similar stabilization of linear isomer is observed in the presence of CH_3Cl, as seen in (Figures S47a and b). From these analyses, it could be inferred that H-acceptor solvents favor branched isomers, while H-donor solvents generate linear isomers.

Natural bond orbital (NBO) analysis can be used to estimate these stabilizing effects theoretically. NBO analysis was used to calculate the second-order perturbation energy E(2) to explain the solvent's stabilization effect over all possible enamine conformers.[50] The NBO analysis is a useful tool for determining not only bonding and anti-bonding interactions but also charge transfer and inter and intramolecular bonding interactions.[51] This can be accomplished by taking into account all possible interactions between filled donor and empty acceptor NBOs, occupied lewis-type (donor) NBOs, and unoccupied non-lewis-type (acceptor) NBOs (see Table S4). Equation (1) gives the stabilization energy E(2) associated with electron delocalization between donor (i) and acceptor (j).

$$\mathrm{E}(2) = \Delta \mathrm{E}_{ij} = \frac{q_i F_{ij}^2}{\left(\varepsilon_i - \varepsilon_j\right)}, \tag{1}$$

where q_i represents donor orbital occupancy, E_i and E_j represent the donor and acceptor orbital energies, respectively, and F_{ij} is the off-diagonal NBO Fock matrix element. Table S4 displays the results of the second-order perturbation theory analysis of the Fock matrix at the ωB97X-D/6-311G(d,p) level of theory. The prominent interactions between Lewis and non-Lewis orbitals of all TS in the solvent phase are thoroughly investigated for a representative H-donor solvent (DMSO) and H-acceptor solvent ($CHCl_3$). The prominent interactions in the DMSO solvent phase show that the syn-branched conformer has the highest E(2) value at 2.09 kcal mol^{-1}. The most prominent interaction in the solvent phase was from a lone pair orbital on O(41) to the anti-bonding acceptor BD * (1) C2-H4 orbital. In the $CHCl_3$ solvent, the syn-linear conformer has the highest E(2) value at 5.06 kcal mol^{-1}, causing higher stabilization energy to these transition states. The most prominent interaction in the solvent phase was from a lone pair orbital on O(19) to the antibonding acceptor BD * (1) C1–H2 orbital.

3.2 *Formation of enantioselective Mannich base from enamine*

The enamine formed in the earlier step generates an H-bonded complex **5** with the cyclic imine benzoxazinone. The intermediate **5** undergoes a conjugate addition to the benzoxazinone, thereby making the nitrogen of benzoxazinone highly nucleophilic. This nitrogen of the benzoxazinone efficiently abstracts the proton from the carboxylic acid group contained in the enamine. Both the above steps are obtained as concerted steps and lead to the formation of zwitterionic moiety **6** as depicted in Scheme 3 concerning the formation of branched product and Scheme S1 of SI associated with the formation of the linear product.

The carbocation formed in **6** is stabilized by the lone pairs of nitrogen, resulting in the formation of an iminium ion. Hydrolysis of iminium ion **6** leads to forming **7**, followed by a proton transfer, which enables the formation of the Mannich base **8** along with the regeneration of the L-proline organocatalyst (Figure 4).

The conjugate addition of **5** to the benzoxazinone, followed by the proton abstraction from the carboxylic acid group contained in the enamine, is the stereoselective step of the reaction. The origin of stereoselectivity is based on the mode of addition of enamine to the benzoxazinone. The backside attack forms the R enantiomer, whereas the front-side attack leads to the generation of the S enantiomer. On exploring the energies involved in the reaction in the presence of DMSO, we observed the R-isomer of **5** to be stable over the S-isomer. The energy barrier involved in forming this stereoselective step is for the R-path with 11.97 kcal mol^{-1}, whereas 15.3 kcal mol^{-1} for the S-path. The TS for the R-isomer is stable over the TS for the S-isomer by 7.96 kcal mol^{-1}. According to the Curtin–Hammett principle, a stable conformer leads to the major or exclusive product if the reaction rate of the stable conformer is higher than that of the less stable one.[52] Therefore, the R-conformer of the product is formed as the major product as the barrier involved in its formation is less, and the rate of formation is also high as compared to the S-conformer. This stabilization of TS of R-isomer is due to the stronger C–H···O interaction of 2.34 Å between O(47) and H(24) as compared to 2.55 Å between O(47) and H(24) of TS of S-isomer as seen in Figure S48(a) and (b), respectively.

Moving on to investigate the energies for the reaction involving the formation of a linear Mannich base, we observed the R-isomer of **5′** to be stable over the

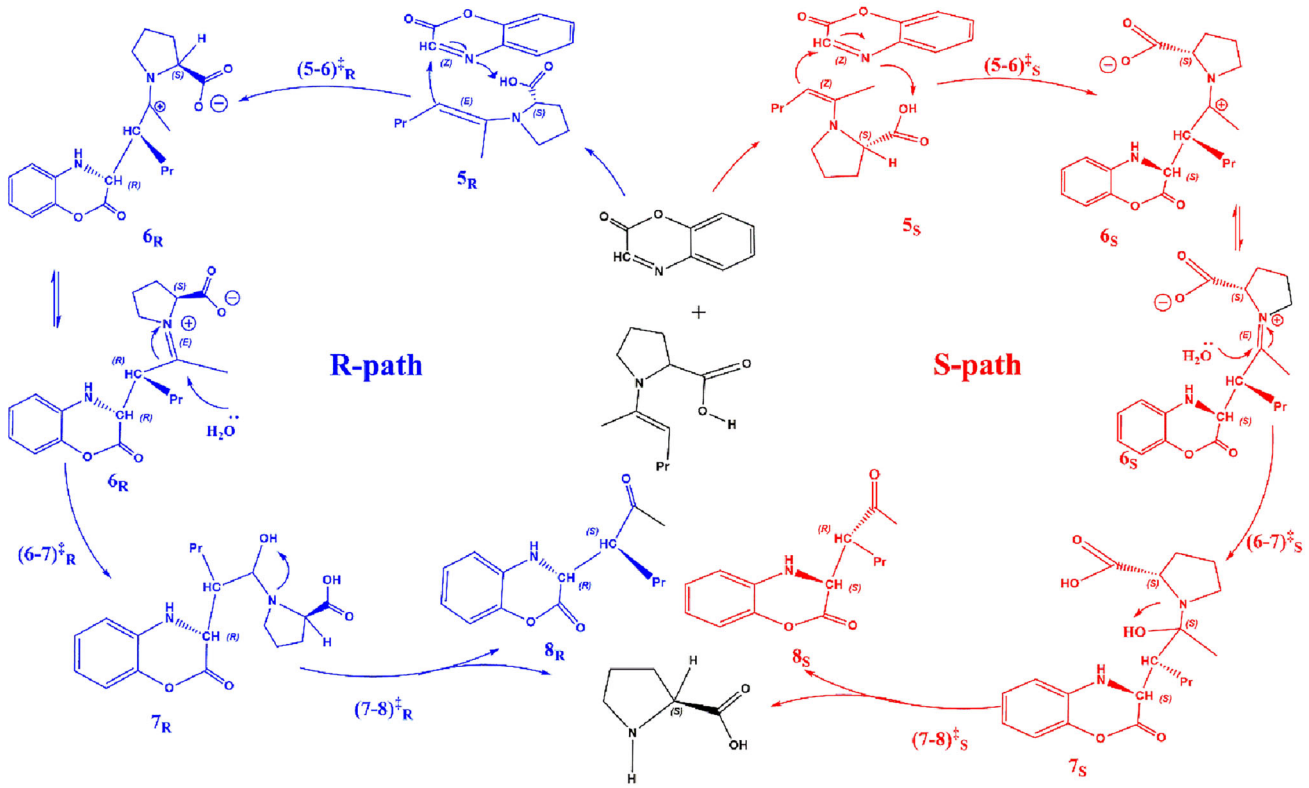

Scheme 3. Formation of branched Mannich base.

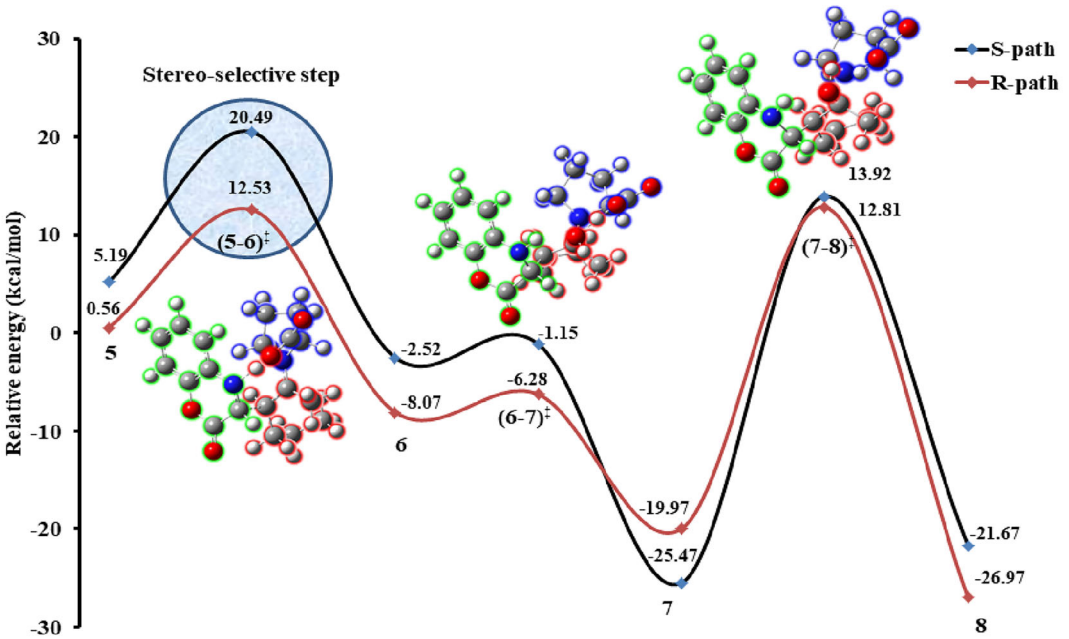

Figure 4. The potential energy figure for the formation of the branched Mannich base, obtained through the electronic energies performed at ωB97X-D/6-311G(d,p) level of theory. The black line indicates the formation of the Mannich base through the S-path, and the brown line represents the formation of the Mannich base through the R-path.

S-isomer. The energy barrier involved in forming this stereoselective step for the R-path is 10.51 kcal mol^{-1}, whereas 18.99 kcal mol^{-1} for the S-path (see Figure S49). The TS for the R-isomer is stable over the TS for the S-isomer by 7.57 kcal mol^{-1}. Figure S48(c) and (d) depict the relatively stable C–H···O interaction with H-bond length of 2.84 Å between O(49) and H(21) in the TS of the R-isomer, compared to 2.93 Å in the TS of the S-isomer, contributes towards the stabilization of the TS of the R-isomer. Since the barrier involved in forming the R-conformer of the product is less and the rate of formation is also high compared to the S-conformer, the R-conformer gets formed as the major product.

Table 2. Theoretically, estimated %ee when DMSO and $CHCl_3$ are obtained at ωB97X-D/6-311G(d,p) level of theory when DMSO and $CHCl_3$ are used as the solvent.

Parameters	Branched Mannich base	Linear Mannich base
$\Delta G_R^{\neq}$	13.21	10.44
$\Delta G_S^{\neq}$	15.54	19.13
$\delta\Delta G^{\neq}$	−2.34	−8.68
Theoretically computed %ee	96	99
Experimentally observed %ee	99[24]	99[24]

Note: Energies reported in the above table are in kcal mol^{-1}.

3.3 *Estimating percent enantiomeric excess for generation of Mannich base*

Enantiomeric excess is a quantitative measure of the excess of one enantiomer over the other in a mixture of enantiomers. The following mathematical equation is used to estimate the percent enantiomeric excess (%ee):[53]

$$\%\,\mathrm{ee} = \frac{\exp\left(-\frac{\delta\Delta G^{\neq}}{RT}\right) - 1}{\exp\left(-\frac{\delta\Delta G^{\neq}}{RT}\right) + 1} \times 100, \qquad (2)$$

where $\delta\Delta G^{\neq} = \Delta G^{\neq}_{\mathrm{RHS}} - \Delta G^{\neq}_{\mathrm{LHS}}$.

The Gibbs free energies listed in Table 2 are considered to compute the percent enantioselectivity (%ee). The TS involved in the formation of the R-enantiomer is stable as compared to the S-enantiomer of the branched Mannich base by 2.34 kcal mol^{-1}. Likewise, in the case of the formation of linear Mannich base, the TS involved in the formation of the R-enantiomer is stable as compared to the S-enantiomer by 8.68 kcal mol^{-1}. The calculated %ee for the formation of the R-enantiomer of the linear Mannich base is >99%. The above-calculated values of %ee are in close agreement with the experimentally reported values of Viji *et al.*[24] Also, our calculations predict the greater yield of formation of linear product as

compared to branched product, which is in line with the experimental findings.

4. Conclusion

The origin of stereo-selectivity, the reaction mechanism, and the role of solvent in the L-proline-catalyzed reaction between benzoxazinone and 2-hexanone have all been computationally explored. The switching of regioselectivity has been displayed due to site-specific solvent interaction with iminium ions. Solvents such as DMSO, THF, and DMF participate as H-acceptors and bind to α-hydrogen atoms of the iminium group. This facilitates the reactivity at the more hindered site, resulting in the formation of a branched isomer. On the other hand, solvents such as $CHCl_3$, CH_2Cl_2, and CH_3Cl participate as H-donors and bind to the carboxylate group of iminium ions. This enables the reactivity to proceed from the less hindered C-chain, leading to a linear isomer. The kinetically stable enamine further reorganizes to form the thermodynamically favored enamine by rotating syn to anti-enamine isomer. Thus, the regioselectivity is induced in the enamines due to solvent-specific interactions. Hence, we observe the formation of anti-branched enamine in H-acceptor solvents and anti-linear enamine in H-donor solvents. These enamines later undergo a conjugate addition with benzoxazinone, leading to an enantioselective Mannich base.

Acknowledgment

The authors acknowledge the Department of Chemistry at the University of Mumbai for making this work feasible.

References

1. Viji M, Lanka S, Sim J, Jung C, Lee H and Vishwanath M 2021 *Regiodivergent organocatalytic reactions Catalysts* **18** 1013
2. Bhattacharjee D, Kshiar B and Myrboh B 2016 L-Proline as an efficient enantioinduction organo-catalyst in the solvent-free synthesis of pyrazolo[3,5-b]quinoline derivatives *via* one-pot multi-component reaction *RSC Advances* **98** 95944
3. Felder S, Wu S, Brom J, Micouin L and Benedetti E 2021 Enantiopure planar chiral [2.2]paracyclophanes: Synthesis and applications in asymmetric organocatalysis *Chirality* **9** 506
4. Bures J, Armstrong A and Blackmond D G 2016 Explaining anomalies in enamine catalysis: 'Downstream species' as a new paradigm for stereocontrol *Acc. Chem. Res.* **2** 214
5. Lu Z, Hammond G B and Xu B 2020 Revisiting the role of acids and hydrogen bond acceptors in enamine formation *Org. Biomol. Chem.* **35** 6849
6. Patil M P and Sunoj R B 2007 Insights on co-catalyst-promoted enamine formation between dimethylamine and propanal through ab initio and density functional theory study *J. Org. Chem.* **22** 8202
7. Mannich C and Krosche W 1912 About a condensation product of formaldehyde, ammonia and antipyrine *Archiv. Der. Pharmazie* **1** 647
8. Bahmanyar S and Houk K N 2001 The origin of stereoselectivity in proline catalyzed intramolecular aldol reactions *J. Am. Chem. Soc.* **51** 12911
9. Blicke F F 2011 The Mannich Reaction *Org. React.* **1** 303
10. Cordova A, Watanabe S, Tanaka F, Notz W and Barbas C F 2002 A highly enantioselective route to either enantiomer of both α- and β-amino acid derivatives *J. Am. Chem. Soc.* **9** 1866
11. Hajos Z G and Parrish D R 1974 Asymmetric synthesis of bicyclic intermediates of natural product Chemistry *J. Org. Chem.* **12** 1615
12. List B, Lerner R A and Barbas C F 2000 Proline-catalyzed direct asymmetric aldol reactions *J. Am. Chem. Soc.* **10** 2395
13. Bock D A, Lehmann C W and List B 2010 Crystal structures of proline derived enamines *PNAS* **48** 20636
14. Allemann C, Gordillo R, Fernando R C, Cheong P and Houk K N 2004 Theory of asymmetric organocatalysis of aldol and related reactions: rationalizations and predictions *Acc. Chem. Res.* **8** 558
15. Fernando R C and Houk K N 2004 Computational evidence of the enamine mechanism of intramolecular aldol reactions catalyzed by proline *Angew. Chem.* **43** 5766
16. Schreiner P R 2003 Metal-free organocatalysis through explicit hydrogen bonding interactions *Chem. Soc. Rev.* **5** 289
17. Seebach D, Beck A K, Badine D M, Limbach M, Eschenmoser A, Treasurywala A M, *et al.* 2007 Are oxazolidinones really unproductive, parasitic species in proline catalysis? thoughts and experiments pointing to an alternative view *Helv. Chim. Acta* **3** 425
18. Sharma A K and Sunoj R B 2010 Enamine versus oxazolidinone: What controls stereoselectivity in proline-catalyzed asymmetric aldol reactions *Angew. Chem. Int. Ed.* **36** 6373
19. Sunoj R B 2011 Proline-derived organocatalysis and synergism between theory and experiments *Comput. Mol. Sci.* **6** 920
20. Haindl M H, Hioe J and Gschwind R M 2015 The proline enamine formation pathway revisited in dimethyl sulfoxide: Rate constants determined via NMR *J. Am. Chem. Soc.* **40** 12835
21. Enders D and Seki A 2002 Proline-catalyzed enantioselective michael additions of ketones to Nitrostyrene *Synlett.* **1** 26
22. Mase N, Nakai Y, Ohara N, Yoda H, Takabe K, Tanaka F and Barbas C F III 2006 Organocatalytic direct asymmetric aldol reactions in water *J. Am. Chem. Soc.* **3** 734

23. Hahn B T, Fröhlich R, Harms K and Glorius F 2008 Recent advances on organocatalysed asymmetric Mannich reactions *Angew. Chem. Int. Ed.* **51** 9985
24. Viji M, Sim J, Li S, Lee H, Oh K and Jung K J 2018 Organocatalytic and regiodivergent mannich reaction of ketones with benzoxazinones *Adv. Synth. Catal.* **23** 4464
25. Gawade P M, Khose V N, Badani P M, Hasan M, Kaabel S, Shaikh M M, *et al*. 2019 Benzyne-mediated nonconcerted pathway toward synthesis of sterically crowded [5]- and [7]oxahelicenoids, stereochemical and theoretical studies, and optical resolution of helicenoids *J. Org. Chem.* **2** 860
26. Kamble S B, Maliekal P J, Dharpure P D, Badani P M and Karnik A V 2020 Synthesis of concave and vaulted 2*H*-pyran-fused BINOLs and corresponding [5] and [7]-oxa-helicenoids: Regioselective cascade-concerted route and DFT Studies *J. Org. Chem.* **12** 7739
27. Gulvi N, Patel P and Badani P M 2018 Exploring unimolecular dissociation kinetics of ethyl dibromide through electronic structure calculations *Chem. Phys.* **505** 55
28. Gaussian 09, Revision A, Frisch M J, Trucks G W, Schlegel H B, Scuseria G E, Robb M A, Cheeseman J R, *et al.* 2009 Gaussian, Inc., Wallingford C T
29. Chai J and Gordonb M H 2008 Systematic optimization of long-range corrected hybrid density Functionals *J. Chem. Phys.* **8** 084106
30. Soleymani M 2019 A density functional theory study on the [3 + 2] cycloaddition of *N*-(*p*-methylphenacyl)benzothiazolium ylide and 1-nitro-2-(*p*-methoxyphenyl) ethene: the formation of two diastereomeric adducts via two different mechanisms *Theor. Chem. Acc.* **7** 87
31. Musawwir A, Farhat A, Khera R A, Ayub A R and Iqbal J 2021 Theoretical and computational study on electronic effect caused by electron withdrawing/electron-donating groups upon the coumarin thiourea derivatives *Comput. Theor. Chem.* **1201** 113271
32. Nakliang P, Yoon S and Choi S 2021 Emerging computational approaches for the study of regio- and stereoselectivity in organic synthesis *Org. Chem. Front.* **18** 5165
33. Lu T and Chen F J 2012 Multiwfn: A multifunctional wavefunction analyser *Comput. Chem.* **5** 580
34. Humphrey W, Dalke A and Schulten K 1996 VMD: Visual molecular dynamics *J. Molec. Graphics* **1** 33
35. Hajos Z G and Parrish D R 1973 Synthesis and conversion of 2-methyl-2-(3-oxobutyl)-1,3-cyclopentanedione to the isomeric racemic ketols of the [3.2.1]bicyclooctane and of the perhydroindane series *J. Org. Chem.* **12** 1612
36. Cordova A, Notz W and Barbas C F III 2001 Proline-catalyzed one-step asymmetric synthesis of 5-hydroxy-(2*E*)-hexenal from acetaldehyde *J. Org. Chem.* **1** 301
37. Bahmanyar S and Houk K N 2001 The origin of stereoselectivity in proline-catalyzed intramolecular aldol reactions *J. Am. Chem. Soc.* **51** 12911
38. Filarowski A and Koll A 1996 Integrated intensity of OH absorption bands in bent hydrogen bonds in *ortho*-dialkylaminomethyl phenols *Vib Spectrosc.* **1** 15
39. Fernando R C and Houk K N 2005 Theoretical studies of stereoselectivities of intramolecular aldol cyclizations catalyzed by amino acids *J. Am. Chem. Soc.* **32** 11294
40. Glendening E D, Landis C R and Weinhold F 2012 Natural bond orbital methods *WIREs Comput. Mol. Sci.* **1** 1
41. Breneman C M and Kenneth B 1990 Determining atom-centered monopoles from molecular electrostatic potentials. The need for high sampling density in formamide conformational analysis *J. Comput. Chem.* **3** 361
42. Maliekal P J, Gulvi N R, Karnik A V and Badani P M 2020 Origin and turnaround of enantioselectivity in a chiral organocatalysed Diels-Alder reaction: A mechanistic study *J. Phys. Org. Chem.* **9** e4072
43. Lu Y, Li H, Zhu X, Zhu W and Liu H 2011 How does halogen bonding behave in solution? A theoretical study using implicit solvation model *J. Phys. Chem. A* **17** 4467
44. Marsden S R, Mestrom L, McMillan D G G and Hanefeld U 2020 Thermodynamically and kinetically controlled reactions in biocatalysis – from concepts to perspectives *Chem. Cat. Chem.* **2** 426
45. Parasuk W and Parasuk V 2008 Theoretical investigations on the stereoselectivity of the proline catalyzed mannich reaction in DMSO *J. Org. Chem.* **23** 9388
46. Reichardt C 2004 *Solvents and solvent effects in organic chemistry* third edition, Wiley, ISBN: 3-527-30618-8
47. Das M, Ranjan A and Sunoj R B 2022 Molecular insights on solvent effects in organic reactions as obtained through computational chemistry tools *J. Org. Chem.* **3** 1630
48. Wei Q, Zhou D, Li X, Chen Y H and Bian H 2018 Structural dynamics of dimethyl sulfoxide aqueous solutions investigated by ultrafast infrared spectroscopy: Using thiocyanate anion as a local vibrational probe *J. Phys. Chem. B* **50** 12131
49. Ho J, Zheng J, Paneda R M, Truhlar D G, Ko E J, Savage G P, *et al.* 2013 Chloroform as a hydrogen atom donor in barton reductive decarboxylation reactions *J. Org. Chem.* **13** 6677
50. Patel P, Lingayat S, Gulvi N and Badani P 2018 Mechanistic and kinetic insights of reduction of indophenol by sodium borohydride: A theoretical study to explore the effect of solvent and counter ion *Chem. Phys.* **504** 13
51. Vik E C, Li P, Pellechia P J and Shimizu K D 2019 Transition-state stabilization by $n \rightarrow \pi^*$ interactions measured using molecular rotors *J. Am. Chem. Soc.* **42** 16579
52. Chakraborty S and Saha C 2016 The Curtin-Hammett principle *Reson.* **2** 151
53. Raghavan B S 2016 Transition state models for understanding the origin of chiral induction in asymmetric catalysis *Acc. Chem. Res.* **5** 1019